Available online at www.sciencedirect.com
SCIENCE DIRECT®
Global and Planetary Change 36 (2003) 117–136
GLOBAL AND PLANETARY CHANGE
www.elsevier.com/locate/gloplacha

Paleoprecipitation estimates for the Lake Naivasha basin (Kenya) during the last 175 k.y. using a lake-balance model

A.G.N. Bergner *, M.H. Trauth, B. Bookhagen

Institut für Geowissenschaften, Universität Potsdam, Postfach 601553, D-14415 Potsdam, Germany

Received 20 August 2001; accepted 19 July 2002

Abstract

We modeled the two most extreme highstands of Lake Naivasha during the last 175 k.y. to estimate potential precipitation/evaporation changes in this basin. In a first step, the bathymetry of the paleolakes at ~ 135 and 9 k.y. BP was reconstructed from sediment cores and surface outcrops. Second, we modeled the paleohydrologic budget during the highstands using a simplified coupled energy mass-balance model. Our results show that the hydrologic and hence the climate conditions at ~ 135 and 9 k.y. BP were similar, but significantly different from today. The main difference is a ~ 15% higher value in precipitation compared to the present. An adaptation and migration of vegetation in the cause of climate changes would result in a ~ 30% increase in precipitation. The most likely cause for such a wetter climate at ~ 135 and 9 k.y. BP is a more intense intertropical convergence and increased precipitation in East Africa.

Keywords: East Africa; Hydrologic modeling; Paleoclimate

1. Introduction

In East Africa, Quaternary climatic changes are recorded in lacustrine sediments reflecting changes in water level and hydrochemistry (e.g., Richardson and Richardson, 1972; Gasse et al., 1989; Johnson et al., 2000; Talbot and Lærdal, 2000; Verschuren et al., 2000; Barker et al., 2001; Trauth et al., 2001). To determine the magnitude of such climate changes, lake-balance modeling is now a widely used and accepted tool (e.g., Barron and Moore, 1994; Nicholson and Yin, 2001). Since the water storage of a lake is directly related to regional hydrologic conditions, these models provide important insights into the relationship between various components of the catchment (i.e., basin geometry, climate, vegetation and subsurface conditions) and can, therefore, also be used to predict future freshwater supply.

Lake-balance models have to be adjusted to the environmental conditions in the basin. This calibration is more precise if several natural scenarios in the same basin are available for different time slices. Unfortunately, instrumental climate records in East Africa are short and do not document the full natural variability in a lake basin. Moreover, the interference of natural changes and human impact on lake-level fluctuations

* Corresponding author. Tel.: +49-331-977-2908; fax: +49-331-977-5060.
E-mail address: bergner@geo.uni-potsdam.de (A.G.N. Bergner).

0921-8181/02/$ - see front matter © 2002 Elsevier Science B.V. All rights reserved.
PII: S0921-8181(02)00178-9

during the last hundred years causes further difficulties. To overcome this problem, environmental conditions can be reconstructed using natural climate archives such as lake sediments. Paleoenvironmental data can help to define extreme hydrologic scenarios and the potential magnitude of precipitation/evaporation changes in the catchment. In such an environment, water-balance modeling provides the opportunity to give precise answers about the absolute values of climate changes in the past.

Widespread lacustrine deposits in the Naivasha basin record multiple lake-level highstands and intermittent lowstands during the last 175 k.y. (Richardson and Richardson, 1972; Richardson and Dussinger, 1986; Trauth and Strecker, 1996; Trauth et al., 2001) (Figs. 1 and 2). High-precision $^{40}Ar/^{39}Ar$ age data of intercalated tuffs provide a precise age control for these hydrological changes. The two most extreme highstands during the last 175 k.y. occurred during the late Pleistocene between 139 and 133 k.y. BP and in the early Holocene between 10 and 6 k.y. BP (Richardson and Richardson, 1972; Trauth et al., 2001). Although timing and magnitude of the hydrologic changes are well known, the climate conditions during these times are not well defined. Results from earlier lake-balance modeling for the early Holocene wet period contradict in the magnitude of climate changes and suggest an increase in precipitation by 10–17% (Hastenrath and Kutzbach, 1983) or 20–55%, respectively (Vincent et al., 1989). For the late Pleistocene, the climate conditions for East Africa have to be interpolated from large-scale general circulation model (GCM) results that suggest changes in the same order of magnitude (Prell and Kutzbach, 1987; deNoblet et al., 1996; Dong et al., 1996). To obtain a more precise estimate for the hydrologic variability in the Central Kenya Rift, we reconstructed the geometry of the water body of Lake Naivasha at around 135 and 9 k.y. BP. Using a water-balance model, we show that a significantly higher precipitation/evaporation ratio is the most likely cause for these two highstands.

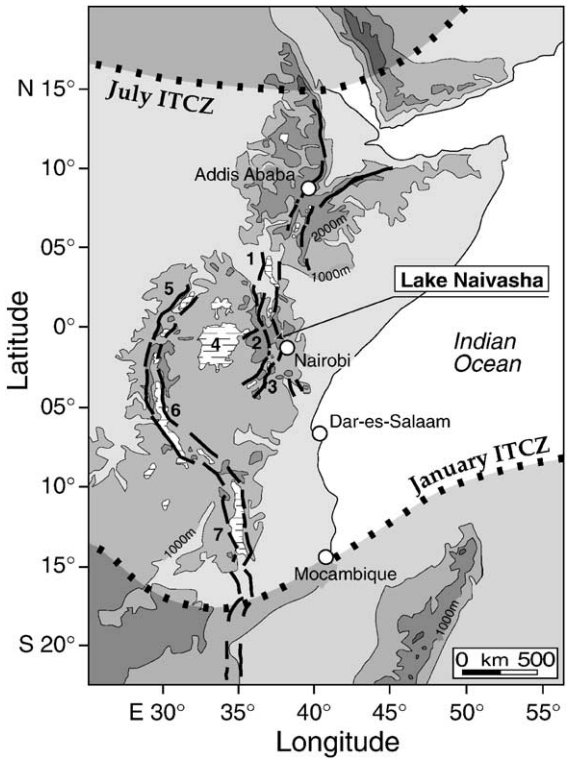

Fig. 1. Topographic map of East Africa showing the major fault systems, the large lakes, the position of the July and January Intertropical Convergence Zone (ITCZ) and the location of the study area. (1) Lake Turkana, (2) Lake Magadi, (3) Lake Natron, (4) Lake Victoria, (5) Lake Albert, (6) Lake Tanganyika, (7) Lake Malawi.

2. Regional settings

Temporal variances in the hydrologic budget of the Central Kenya Rift lakes are mainly controlled by changes in precipitation, which is in turn linked to the seasonal migration of the Intertropical Convergence Zone (ITCZ) (Nicholson, 1996). This pronounced equatorial low-pressure cell is caused by the zenith of the overhead sun and, therefore, reaches its maximum value during March and September in the Central Kenya Rift. While surface temperatures coincide with maximum solar radiation, the time of maximum rainfall follows the latitudinal position of the ITCZ with a time lag of about 4 weeks. Local rainfall mainly results from moisture transport from the Indian Ocean and/or westerly winds from the Congo basin (Fig. 3). Both wind circulation systems are attracted by the ITCZ, crossing East Africa and causing convective rainfall in the center of the ITCZ. Heaviest rains occur in spring, when the trade winds

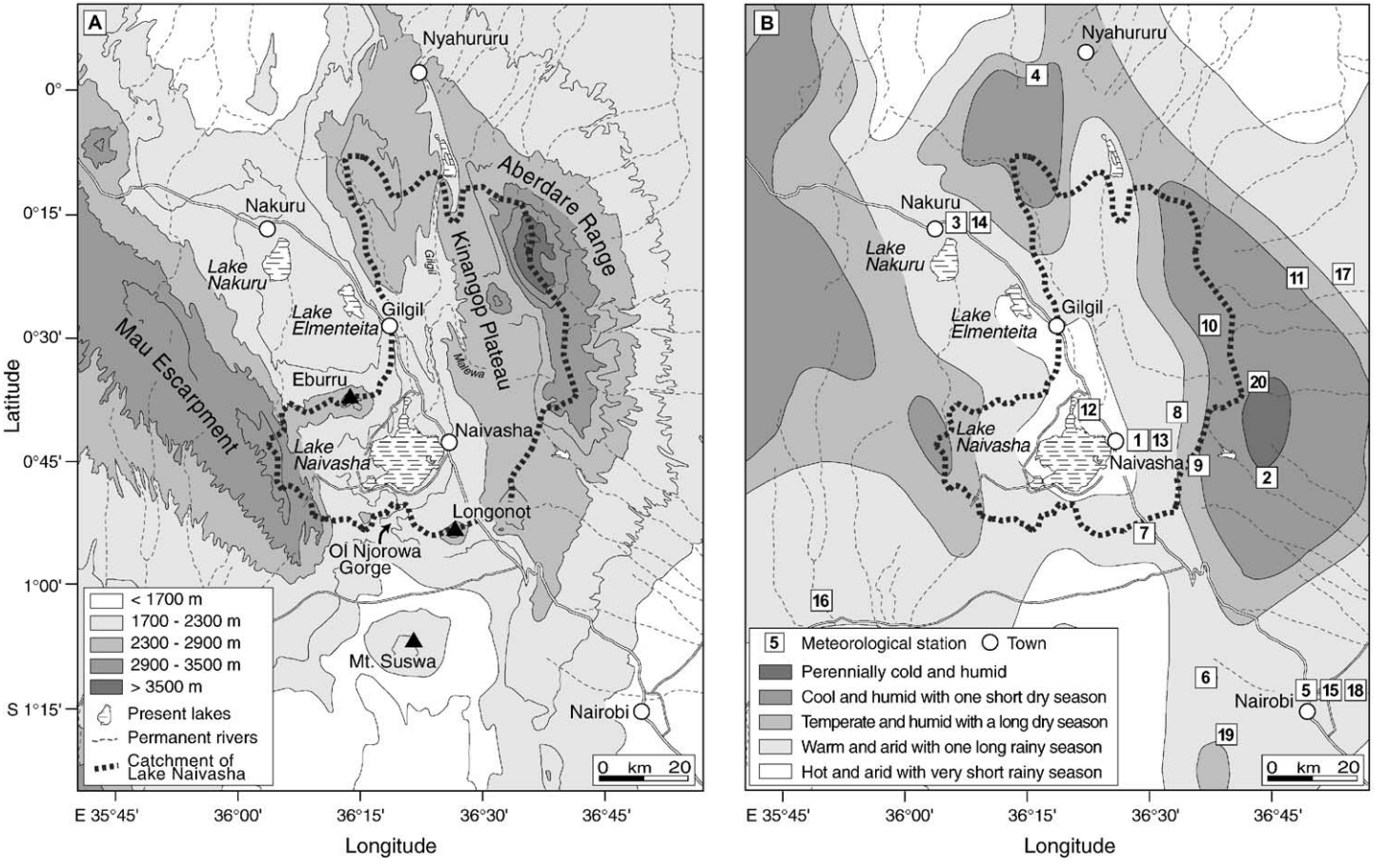

Fig. 2. Map of the Naivasha basin in the Central Kenya Rift showing (A) topography and (B) climate conditions in the lake catchment area and locations of meteorological stations: (1) Naivasha W.D.D., (2) Kimakia Forest Station, (3) Nakuru Met. Station, (4) Nyahuhuru, (5) Nairobi Dagoret Corner, (6) Muguga K.A.R.I., (7) Kedong Ranch, (8) Naivasha Mkungi, (9) Longonot Carnell, (10) Aberdare West Gate, (11) Aberdare East Gate, (12) Naivasha Morendat, (13) Naivasha Kongoni Farm, (14) Nakuru, (15) Nairobi Internatinal Airport, (16) Narok, (17) Nyeri, (18) Kiambu, (19) Ngong, (20) S. Kinangop (Ndiara). Climate information from KMD (2000) (stations 1–7), Vincent et al. (1989) (stations 8–11, 13), Vincent et al. (1979) (station 12), GDS (1994) and ISMCS (1995) (stations 14–17), Rodhe and Virji (1976) (stations 18–19), Ojany and Ogendo (1988) (station 20).

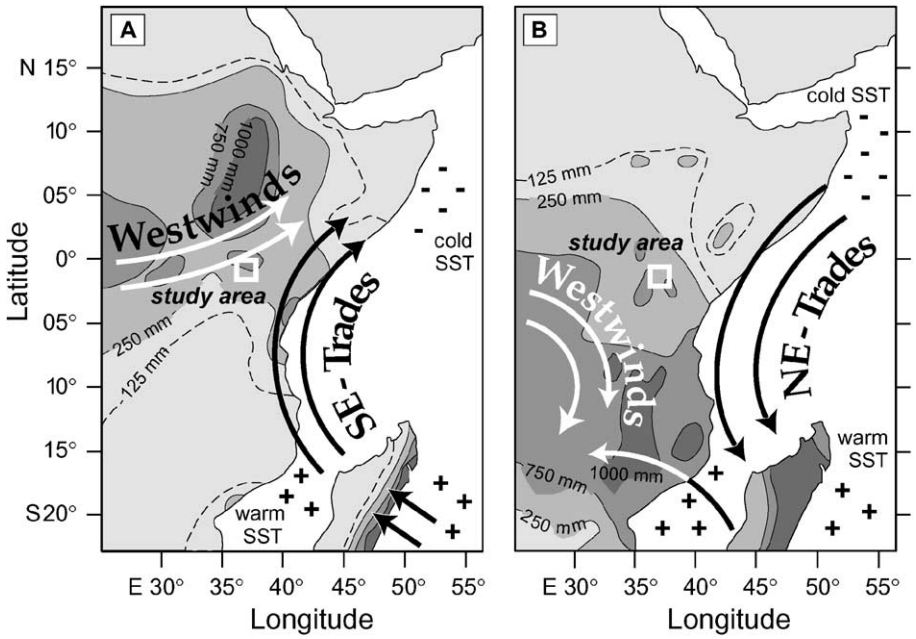

Fig. 3. Air flow pattern and precipitation of East Africa during (A) May to October and (B) November to April. Contours of seasonal precipitation show rainfall maxima in northern (Ethiopia) and southern East Africa (Madagascar), which are manly controlled by topography and sea-surface temperatures (SST) of the Indian Ocean. The predominating circulation systems of the SE and NE trade winds, as well as westwind streams, only indirectly affect the rainfall pattern of the study area. Modified after Survey of Kenya (1991).

parallel the rift margins and thunderstorms occur every afternoon.

Located at 1890 m above sea level, Lake Naivasha is the highest lake in the Central Kenya Rift (0°55′ S 36°20′ E) (Fig. 2). The Mau Escarpment (3080 m a.s.l.) and the volcano Mt. Eburru (2840 m) bound the closed-basin lake to the west. To the north and east (Kinangop Plateau), the basin is bordered by Plio-Pleistocene fault scarps, whereas the volcano Mt. Longonot (2776 m) and the Olkaria Volcanic Complex (2440 m) define a southern barrier. The history of the Naivasha basin began at about 320 k.y. BP, when lava flows at Olkaria closed the southern outlet between the flanks of the 400-k.y.-old Mt. Longonot and the Mau Escarpment. However, a large lake did not exist before ~ 146 k.y. BP (Trauth et al., 2001). Modern Lake Naivasha contains ~ 0.85 km^3 of water and covers an area of about 180 km^2. Around 20% of the lake surface is covered by papyrus swamps. Whereas most of the Kenya Rift lakes such as Lake Elmenteita (1776 m) and Lake Nakuru (1758 m) are highly alkaline, Lake Naivasha is fresh and has a pH of ~ 8.1 (Åse, 1987). Since the lake area only receives 600 mm $year^{-1}$ of rainfall and potential evapotranspiration is about 1900 mm $year^{-1}$ (Clarke et al., 1990), the low pH can only be a consequence of the high water influx from the Malewa and Gilgil rivers draining the Kinangop Plateau and the 4400-m high Aberdare Range to the east. In these areas, evapotranspiration is low due to a thin vegetation coverage up to elevations of 2600 m and high water runoff on steep slopes with poorly developed soils (Griffiths, 1972; Jätzold, 1981; KMD, 2000) (Figs. 2 and 6). In contrast, high elevated afromontane forests of the Aberdare Range play a major role in storing huge amounts of moisture (Jätzold, 1981). As shown by experiments in water wells, almost the entire amount of water received from the rift margins reaches Lake Naivasha after a very short time (e.g., Vincent et al., 1979; Onacha, 2000). Infiltrating into the lake, about 15% of the river input leaves the lake by underground seepage through porous volcanic material. Although the total amount

of this subsurface outflow is still a matter of debate, this process is certainly important in the hydrochemical budget and the solute export from the lake (e.g., Gaudet and Melack, 1981; Ojiambo-Bwire and Lyons, 1996).

3. Methods

The model employed in this study computes an equilibrium lake level of a closed-basin lake using the balance between basin-averaged precipitation and evaporation. As in most lake-balance models, evaporation is the most critical component, but difficult to determine. Our model uses a energy-budget method evaluating incoming and outgoing radiation at the earth's surface. The algorithm was first developed by Blodgett et al. (1997), but significantly modified, translated into Matlab® code and applied to a landslide-dammed lake in the Central Andes by Bookhagen et al. (2001). The most important differences in the application of the model to the semiarid intra-Andean basin and Lake Naivasha were the importance of seepage and a potential vegetation feedback in the lake basin.

The steady state hydrological budget for a closed-basin lake system can be written as:

$$\Delta V_{\text{lake}} = P_{\text{bas}} - [E_{\text{w}}\alpha_{\text{w}} + E_{\text{l}}(1-\alpha_{\text{w}})] - S_{\text{bas}} = 0 \quad (1)$$

where ΔV_{lake} is the volumetric change in the water body, P_{bas} is the basin-averaged precipitation, E_{w} and E_{l} denote the evaporation over water and land, respectively, α_{w} is the lake–area ratio, or the fraction of the catchment covered by water, and S_{bas} is the basin-integrated seepage (Fig. 4). Whereas the modern values for P_{bas}, E_{w} and S_{bas} are easy to determine, E_{l} is difficult to estimate mainly due to the complexity

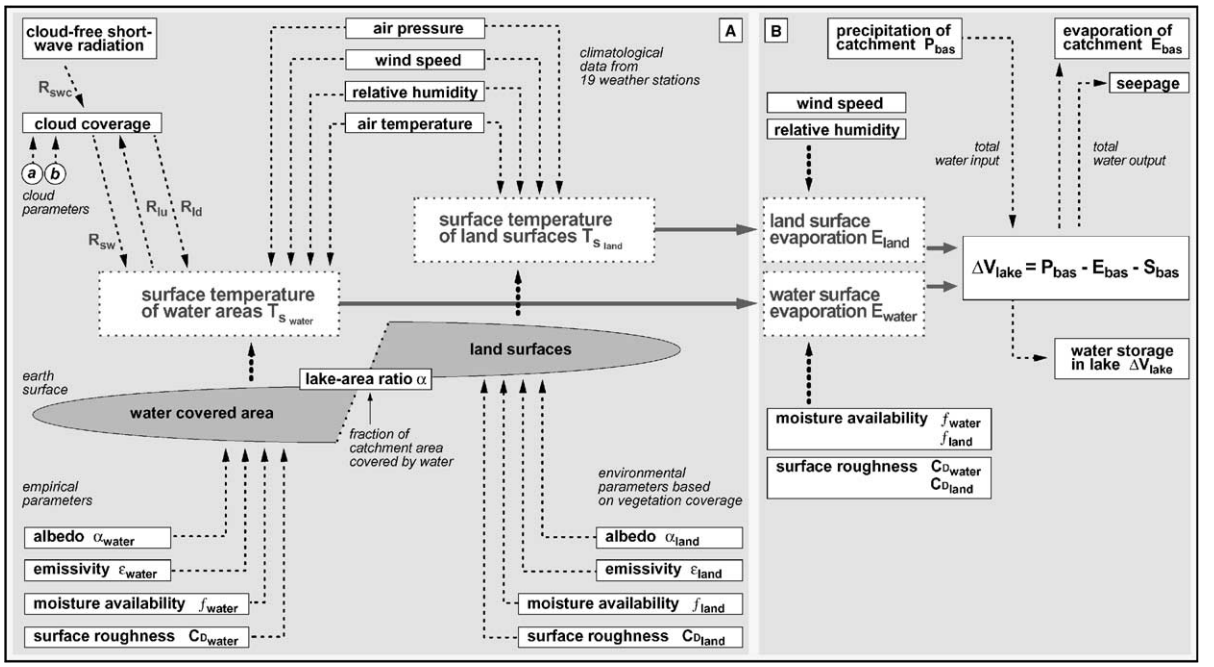

Fig. 4. Concept of lake-balance model based on Blodgett et al. (1997) and Bookhagen et al. (2001) showing the major components of the hydrologic system. The model is a combination of an (A) energy budget approach, where the potential evaporation rate of the earth surface is calculated from radiation-controlled and climate-triggered energy transformations at the lower atmosphere boundary. Based on the differences between water- and vegetation-covered areas, two values of potential evaporation are obtained and introduced into a (B) mass-balance equation. Herein, the total of the catchment evaporation is balanced with the values of basin-averaged precipitation and seepage. In the case of a hydrologic steady state, the change in the water storage of the closed-basin Lake Naivasha is zero.

of related parameters and their spatial variability in the catchment. On the other hand, the equation clearly indicates that higher lake levels and larger lakes are always the consequence of increased precipitation and/or reduced evaporation and seepage, as long as no important tectonic movements affected the basin geometry during the studied time-period.

For the hydrologic modeling, we used a two-step approach. First, the present-day lake was modeled using modern climate parameters. The result was intensely tested for robustness and sensitivity to all parameters. Then, the reconstructed paleolakes were modeled by changing the climate parameters until the paleolake levels were reached. During the modeling, changes in the radiation pattern due to variations in the earth's orbit as well as changes in vegetation in the cause of climate shifts were considered (Kutzbach and Webb, 1993; Kutzbach et al., 1996; Carrington et al., 2001). From all solutions, the scenarios consistent with results from pollen analyses and large-scale GCMs were preferred (e.g., Maitima, 1991; Street-Perrott and Perrott, 1993; deNoblet et al., 1996; Dong et al., 1996).

3.1. Paleolake reconstruction techniques

The chronology of the lake-level fluctuations in the Naivasha basin is based on the correlation of lake-sediment outcrops at 12 locations in the Lake Naivasha basin (Washbourn-Kamau, 1975; Bone, 1985; Clarke et al., 1990; Trauth et al., 2001) (Fig. 5). In the Ol Njorowa Gorge within the southern rim of the basin, a 60-m-thick succession of lake sediments, between 146 and 60 k.y. old, is used as a reference section for the late Pleistocene lake highstands (Trauth and Strecker, 1996). The deposits of the early Holocene highstand were described in a sediment core from the present lake (Richardson and Richardson, 1972; Richardson and Dussinger, 1986) and additional unpublished core logs from water wells (S. Higgins, personal communication, 2000) (Fig. 5).

The geometry of the water body for the 135- and 9-k.y. BP time slices was reconstructed from the elevation of the youngest sediments deposited during these highstands. A set of elevation reference points was obtained by correlating the different outcrops and profiles. The altitude of each reference point was corrected for tectonic movements and erosion using the chronology by Bosworth and Strecker (1997). The typical offsets of normal faults for the last 175 k.y. are in the order of a few meters (Strecker et al., 1990; Bosworth and Strecker, 1997). The reference points were embedded into a digital elevation model (DEM) of the present-day Naivasha basin. Because of their significantly older tectonic history, it is assumed that the higher elevated parts of the catchment were not subjected to important morphological changes during the last 300 k.y. (Baker and Wohlenberg, 1971; Strecker et al., 1990; Bosworth and Strecker, 1997). All present elevation data are based on digitized topographic maps at a scale of 1:250,000 and 1:50,000.

The paleolakes were computed by triangulation between the reference points using bilinear and *t*-spline interpolation techniques. The *t*-spline technique uses Green's functions for a spline in tension (Wessel and Bercovici, 1998). The inclusion of a tension *t* greatly improves the stability of the method relative to conventional gridding routines without tension, e.g., undesirable oscillations between data points. The value of *t* can vary between 0 (corresponding to the biharmonic spline solution; Sandwell, 1987) and 1 equivalent to bilinear interpolation.

3.2. Algorithm for modeling modern and paleoevaporation

The energy budget equation after Brutsaert (1982) and Shuttleworth (1988) assumes that the difference

Fig. 5. Geology of the Naivasha basin. (A) Map showing lithologic units (after Clarke et al., 1990) and key outcrops in the vicinity of the modern lake for paleolake reconstruction. (B) Stratigraphic correlation for bathymetry reconstructions with inferred paleolake levels and corresponding sediments (dashed). (1) Oserian Farm (Washbourn-Kamau, 1975), (2) Munyu railway cut (Washbourn-Kamau, 1975), (3) Lolonito North (Bone, 1985), (4) Ololbutot North (Bone, 1985), (5) Ol Njorowa Gorge (Trauth et al., 2001), (6) Ol Njorowa Gorge II (Clarke et al., 1990), (7) Maasai Gorge (Clarke et al., 1990), (8) Gorge Farm North (Clarke et al., 1990), (9) Lake Naivasha South (Bone, 1985), (10) Lake Naivasha South II (private sediment core by S. Higgins, personal communication, 2000), (11) Crescent Island (Richardson and Richardson, 1972), (12) Naivasha East (unpublished core data by the Kenyan Government, personal communication, 2000), (13) Waterloo Ridge (Clarke et al., 1990), (14) Gilgil railway cut (Washbourn-Kamau, 1975), (15) Malewa railway cut (Washbourn-Kamau, 1975).

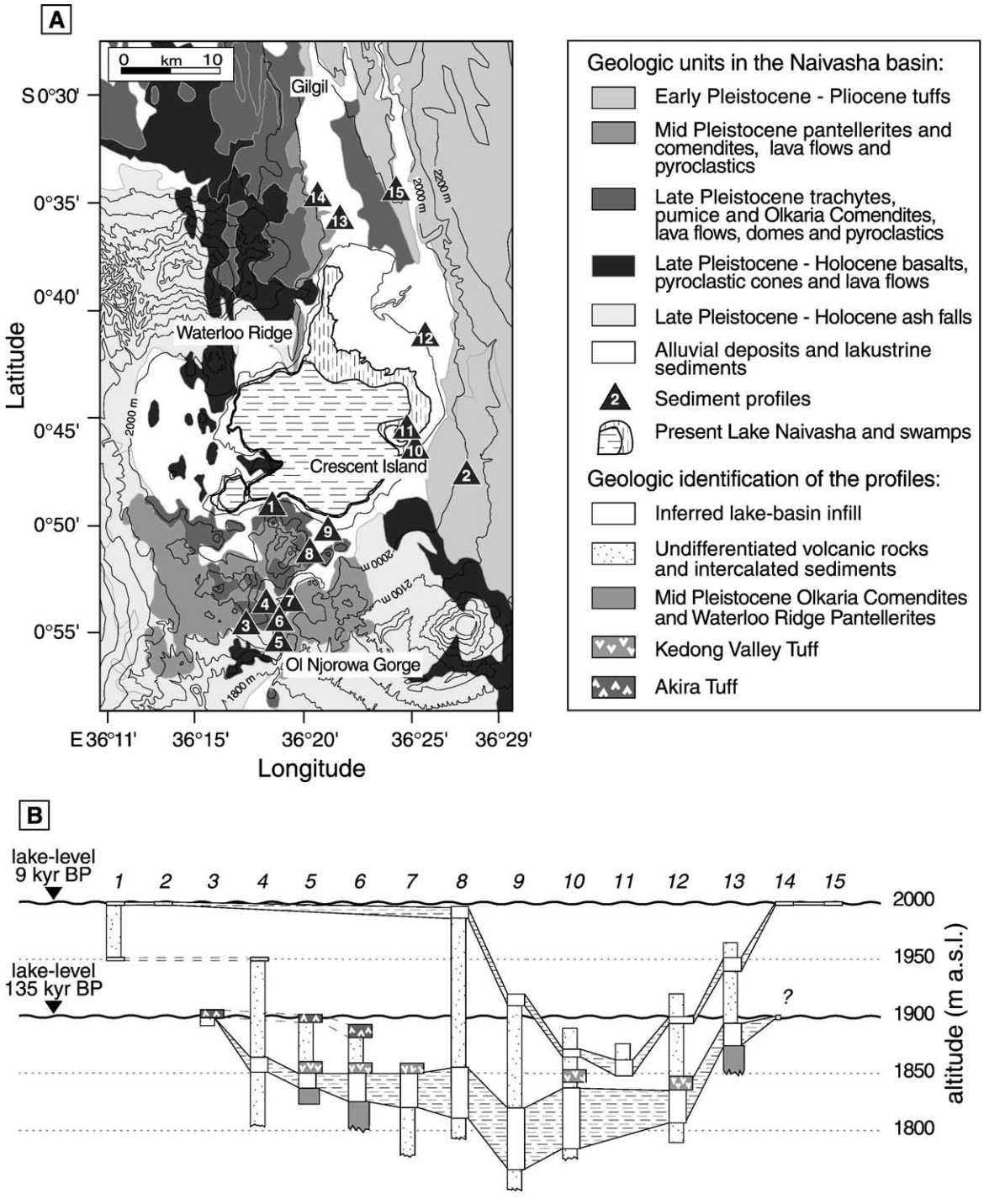
A
0 km 10
Gilgil
Waterloo Ridge
Crescent Island
Ol Njorowa Gorge
2200 m
2000 m
2100 m
1800 m
S 0°30'
0°35'
0°40'
0°45'
0°50'
0°55'
Latitude
E 36°11'
36°15'
36°20'
36°25'
36°29'
Longitude
Geologic units in the Naivasha basin:
Early Pleistocene - Pliocene tuffs
Mid Pleistocene pantellerites and comendites, lava flows and pyroclastics
Late Pleistocene trachytes, pumice and Olkaria Comendites, lava flows, domes and pyroclastics
Late Pleistocene - Holocene basalts, pyroclastic cones and lava flows
Late Pleistocene - Holocene ash falls
Alluvial deposits and lakustrine sediments
Sediment profiles
Present Lake Naivasha and swamps
Geologic identification of the profiles:
Inferred lake-basin infill
Undifferentiated volcanic rocks and intercalated sediments
Mid Pleistocene Olkaria Comendites and Waterloo Ridge Pantellerites
Kedong Valley Tuff
Akira Tuff
B
lake-level 9 kyr BP
lake-level 135 kyr BP
1 2 3 4 5 6 7 8 9 10 11 12 13 14 15
?
2000
1950
1900
1850
1800
altitude (m a.s.l.)

between incoming and outgoing radiation at the earth surface, the net heating rate, is zero:

$$R_{sw} - R_{lu} + \varepsilon R_{ld} - H - LE = 0 \quad (2)$$

where R_{sw} is the net shortwave radiation down, R_{lu} the longwave radiation up, ε the surface emissivity, R_{ld} the longwave radiation down, H the sensible heating rate, L the latent heat of vaporization and E is rate of evaporation. Solving for E, the equation becomes:

$$E = \frac{H - \varepsilon R_{ld} + R_{lu} - R_{sw}}{L} \quad (3)$$

where H is calculated by

$$H = \frac{pC_D U c_p}{RT_a}(T_s - T_a) \quad (4)$$

with p for the air pressure, C_D for the surface drag coefficient, U refers to wind speed, c_p is the specific heat of dry air, R the gas constant of dry air and T_a and T_s corresponding to the air and surface temperature, respectively (Brutsaert, 1982). The net longwave radiation down R_{ld} is obtained by:

$$R_{ld} = 1.24\left[\frac{\mathrm{rh}es(T_a)}{100T_a}\right]^{\frac{1}{7}}\sigma T_s^4(1 - a'\mathrm{cc}^{b'}) \quad (5)$$

where rh is the relative humidity, $es(T_a)$ the saturation vapour pressure depending on temperature, σ reflects the Stefan–Boltzmann constant and a' and b' refer to longwave cloud parameters. The net longwave radiation up R_{lu} can be given as:

$$R_{lu} = \varepsilon\sigma T_s^4 \quad (6)$$

where ε corresponds to the surface emissivity (Brutsaert, 1982). The net shortwave radiation down R_{sw} is calculated from the cloud-free shortwave radiation R_{sws}, the surface albedo α, two values referring to shortwave cloud parameters a and b and the cloud cover cc (Brutsaert, 1982):

$$R_{sw} = R_{swc}(1 - \alpha)[1 - (a + b\mathrm{cc})] \quad (7)$$

Independently from the energy budget equation, the potential evaporation can be calculated using a bulk transfer method as described by Brutsaert (1982):

$$E_{pot} = \frac{0.622C_D U f}{RT_a}[es(T_s) - \mathrm{rh}es(T_a)] \quad (8)$$

where E_{pot} is the potential evaporation and f is the soil moisture availability; both parameters are given in volumetric units.

Combining Eqs. (3) and (8), evaporation in the Naivasha catchment can be estimated from very few environmental parameters. Assuming that radiation-controlled energy transformations at the atmosphere/lithosphere boundary are the triggering mechanism for evaporation from the surface, evaporation clearly depends on the characteristics of the boundary layer. Since the high topographic relief of the 3400-km^2 large Naivasha catchment forces spatially varying environmental conditions, we resampled all parameters to a 1 × 1-km regular grid using t-spline interpolation techniques (Wessel and Bercovici, 1998). Climatic data were obtained by averaging data sets for the last 20 years from 19 weather stations (GDS, 1994; ISMCS, 1995; KMD, 2000) and expanding this dataset by contoured values from climatological maps (Griffiths, 1972; Jätzold, 1981; Ojany and Ogendo, 1988; Survey of Kenya, 1991). The present-day vegetation coverage was obtained from vegetation maps and field observations published by Jätzold (1981), Ojany and Ogendo (1988) and the Survey of Kenya (1991) and additional information from satellite images and field mapping.

Based on basin-averaged values, the modern hydrologic budget for Lake Naivasha was computed using Eq. (1). For the paleoclimatic scenario, the corresponding climate parameters were determined according to orbital-induced insolation changes and limited environmental data such as vegetation reconstructions based on Holocene pollen data (Maitima, 1991; Street-Perrott and Perrott, 1993). For some parameters, such as wind speed and cloud coverage, modeling results from GCM results provided important constraints. Since several parameters were only determined for the 9-k.y., but not for the 135-k.y. BP timeslice, we used the 9-k.y. BP conditions as a starting point also for the late Pleistocene model run.

4. Reconstruction of paleolakes

In contrast to the rift-shoulder areas, i.e., the Aberdare Range and the Mau Escarpment, tectonism and volcanism during the last 300 k.y. significantly modified the inner graben part of the catchment. At around 300 k.y. BP, the inner rift depression reached a maximum altitude near Gilgil (at 2010 m today), separating the Nakuru–Elmenteita and Naivasha basins (Thompson and Dodson, 1963) (Fig. 2). From this point, the rift floor descends north- and southward with a ~2% gradient. Late Pleistocene trachytes, like the Gilgil Trachytes in the North (~950 k.y. old) and the Limuru Trachytes in the South (~2.01–1.88 M.y. old), as well as the Kinangop Tuffs in the East and the Mau Tuffs in the West (~4.5–3.4 M.y. old), were the most prominent geologic units deposited in the inner rift (Clarke et al., 1990). The majority of the mid Pleistocene Olkaria Comendites, the Ol Njorowa Pantellerites and the Olongonot Volcanics were erupted well before 320 k.y. BP closing the Naivasha basin towards the south (Trauth and Strecker, 1996). The volcanic barrier reached a minimum elevation of around 1950 m and was laterally overlain by lake deposits. The base of these lake sediments documents the earliest history of Lake Naivasha after ~146 k.y. BP (Fig. 5).

The 135-k.y. BP highstand is documented by a sequence of lake sediments containing two diatomite beds and intercalated waterlain tuffs. The sequence reaches ~20 m in the Ol Njorowa Gorge and thickens toward the deepest point of the paleolake up to 80 ± 10 m. The sediments are covered by the 106 ± 4-k.y.-old Kedong Valley Tuff (Trauth et al., 2001). This tuff can be easily identified in most of the other outcrops and sediment cores north of the gorge and represents an excellent paleobathymetric marker horizon (Fig. 5). This marker defines the position of the lake bottom at 1840 m in the location of the Ol Njorowa Gorge, descending northward to around 1750 m near the center of the present lake. North of the present Lake Naivasha, lake sediments overlying volcanic rocks of a similar age as the Olkaria volcanic rocks define an elevation of 1875 m for the lake bottom (Clarke et al., 1990). Sedimentary indicators, such as authigenic minerals and diatoms at the southern end of the Ol Njorowa Gorge suggest that the paleolake level remained at around 1900 ± 10 m for a long time span. The large lake deepened toward the center, but expanded into much shallower areas in the south and northeast. This geometry is corroborated by results from diatom analysis indicating shallow- and deep-water environments (Trauth and Strecker, 1996; Trauth et al., 2001).

Taking into consideration that the maximum lake level reached approximately 1900 m, the best approximation for the true paleolake size was obtained using the *t*-spline method with $t = 0.2$. The paleolake then covers an area of about 520 km^2 and the volume of the water body is ~55 km^3 (Table 1). In comparison with the present-day lake, the paleolake was three times larger with a volume of the water body 60 times larger. At its deepest point, the paleolake was 150 m deep, in comparison with 9 m for the present-day lake (Fig. 6).

In contrast to the Pleistocene conditions, the early Holocene morphology of the Naivasha basin was not

Table 1
Summary of reconstructed basin geometry using various interpolation techniques

Method	9-k.y. BP time slice		135-k.y. BP time slice	
	Lake size (km^2)	Volume (km^3)	Lake size (km^2)	Volume (km^3)
t-spline ($t = 0.1$)	693.3	64.9	525.4	57.0
t-spline ($t = 0.2$)	692.6	64.3	**518.5**	**55.4**
t-spline ($t = 0.7$)	**684.5**	**59.3**	472.6	46.8
t-spline ($t = 0.9$)	667.7	54.3 *	442.6 *	40.6 *
Linear with 1×10^{-2} km^2 grid cells	627.6 *	55.1	476.6	45.9
Quintic	697.2	63.6	525.9	56.4
Mean	677.2	60.3	493.6	50.4
Mean without values indicated by (*)	687.1	61.4	503.8	52.3

All calculations were done in Matlab® using 1 × 1-km regular grids of elevation reference points. Values for the size and volume of the paleowater bodies of Lake Naivasha during the 9- and 135-k.y. BP highstands were obtained from different interpolation techniques. *t*-spline interpolation uses Green's functions for a spline in tension (Wessel and Bercovici, 1998), where *t* varies between 0 (equivalent to biharmonic spline solution; Sandwell, 1987) and 1 (equivalent to bilinear interpolation). The quintic method refers to a fifth-order cubic interpolation method. Best estimates for the true paleolake extensions are closest to the median and written in bold letters (*t*-spline interpolation with $t = 0.7$ for the 9-k.y. BP highstand and $t = 0.2$ for the 135-k.y. BP highstand).

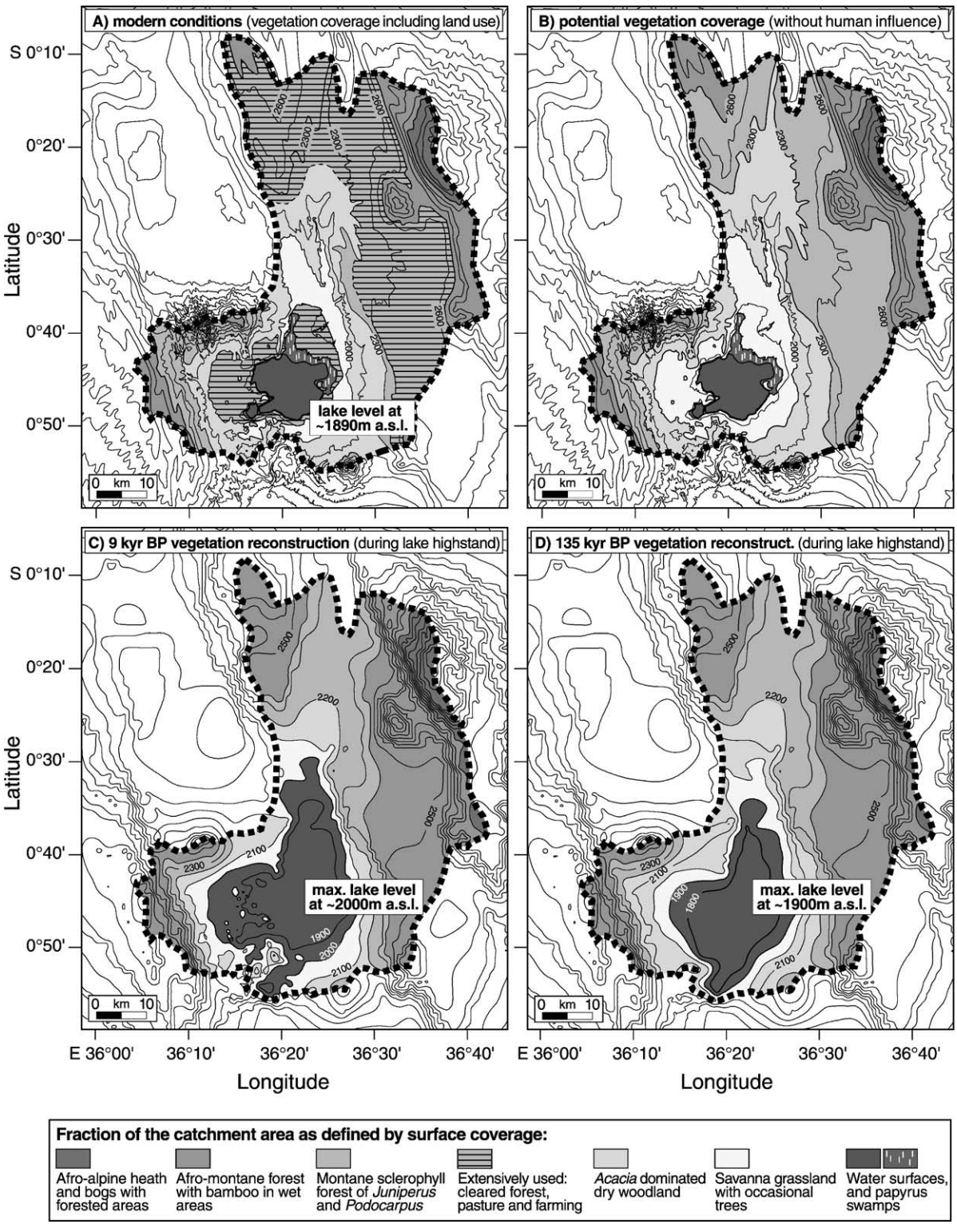
A) modern conditions (vegetation coverage including land use)
B) potential vegetation coverage (without human influence)
C) 9 kyr BP vegetation reconstruction (during lake highstand)
D) 135 kyr BP vegetation reconstruct. (during lake highstand)
lake level at ~1890m a.s.l.
max. lake level at ~2000m a.s.l.
max. lake level at ~1900m a.s.l.
0 km 10
S 0°10'
0°20'
0°30'
0°40'
0°50'
Latitude
E 36°00'
36°10'
36°20'
36°30'
36°40'
Longitude
Fraction of the catchment area as defined by surface coverage:
Afro-alpine heath and bogs with forested areas
Afro-montane forest with bamboo in wet areas
Montane sclerophyll forest of Juniperus and Podocarpus
Extensively used: cleared forest, pasture and farming
Acacia dominated dry woodland
Savanna grassland with occasional trees
Water surfaces, and papyrus swamps

much different from the present-day situation. The activity of the Eburru Volcanic Center and the inner graben volcanoes terminated before the Holocene lake-level highstand. Only a few volcanic centers of the Olkaria Complex erupted after this event (Clarke et al., 1990). The onset of the 9-k.y. BP highstand was documented in a sediment core obtained in the Crescent Island Crater, where deposits of this age were described at ~28 m depth below the present-day lake bottom (Richardson and Richardson, 1972). The 9–6-k.y.-old sediment layer has a thickness of about 14 m at an altitude of 1848–1862 m. Equivalent sediments were neither identified in the Ol Njorowa Gorge nor in the deposits of the Olkaria or Mt. Longonot volcanic complex. Only in the outcrops close to the present shoreline, Holocene lake sediments were identified (Bone, 1985; Clarke et al., 1990; S. Higgins, personal communication, 2000). In addition, beach gravels inferred to correspond to this lake highstand, were found in several localities at an elevation of about 2000 m (Washbourn-Kamau, 1975; Bone, 1985). From morphologic observations and the distribution of lake deposits, we infer that the maximum thickness of these highstand deposits occurs near the deepest point of the present-day Lake Naivasha, and thins out toward the shore lines. The past 6 k.y. BP sediments only slightly modify the early Holocene lake bathymetry, since they are ≤ 20 m thick (Richardson and Richardson, 1972; Clarke et al., 1990) (Fig. 5).

Although beach gravels suggest that the lake remained at the observed elevations for a longer time, a second stable lake occurred at a deeper elevation. At the time when the paleolake reached 2000 m, overflowing water partly eroded the southern barrier and began to form the modern Ol Njorowa Gorge. Subsequently, the lake level dropped gradually, until it stabilized again at about 5700 BP (Richardson and Richardson, 1972). This second stable paleolake level is inferred from paleoshorelines at 1950 ± 10 m (Washbourn-Kamau, 1975). Assuming the maximum Holocene lake level at an elevation of 2000 ± 10 m, the most likely lake size was around 685 km^2. In contrast to the Pleistocene lake reconstructions, the best result was obtained using a *t*-spline interpolation with $t = 0.7$, where the curvature of the modeled bathymetry is at a minimum. The volume of this water body is approximately 59 km^3 (Table 1; Fig. 6). For the lower stable lake level at ~1950 m, the corresponding values were 480 km^2 for the lake area and 34 km^3 for volume.

5. Validation of the hydrologic model for the present-day Lake Naivasha

Due to the high relief and large lateral vegetation changes, the present-day Lake Naivasha basin shows extreme gradients for single environmental parameters (Jätzold, 1981). In order to take into account this spatial heterogeneity, basin-averaged values for the Lake Naivasha catchment were obtained using two different techniques; climatological parameters, such as insolation, precipitation, air pressure, wind speed, cloud coverage, relative humidity and air temperature were calculated by interpolation between climate stations within and in the vicinity of the catchment (Fig. 2). The basin-averaged value for temperature is 13.5 ± 0.5 °C, whereas annual precipitation varies between 950 and 1050 mm $year^{-1}$. Wind speed for the Lake Naivasha basin was obtained from the climatic stations Nyahururu, Nakuru, Naivasha and Nairobi (GDS, 1994; ISMCS, 1995; KMD, 2000). From these data sources, a basin-averaged value of 2.5 ± 0.3 m s^{-1} was determined, which is consistent with results from Nicholson (1996), as well as measurements by R. Hennemann (personal communication, 2001). The solar radiation was set to 415 ± 3 W m^{-2} according to Berger and Loutre (1991); cloudiness was $65 \pm 5\%$ and relative humidity was $65 \pm 5\%$ using the informa-

Fig. 6. Comparison of the modern and reconstructed paleoconditions for Lake Naivasha and the catchment. Upper graphs show the present-day morphology and vegetation coverage compiled from topographic and vegetation maps, satellite images and field observations. Elevation contours were generated at different scales for the outer (1:250,000) and inner (1:50,000) parts of the basin. Whereas the actual vegetation distribution, as shown in (A), was used for the present-day hydrologic modeling, (B) illustrates the estimated modern vegetation coverage without human impact. Paleoreconstructions (lower graphs) were obtained from 3D landscape computations based on geologic field data and *t*-spline interpolation techniques with (C) $t = 0.7$ for 9 k.y. BP highstand and (D) $t = 0.2$ for 135 k.y. BP highstand. Paleovegetation reconstructions are based on published pollen data for the Holocene. The reconstructed 9 k.y. BP vegetation coverage was also applied to the 135 k.y. BP situation, based on significant similarities in the large-scale climate conditions.

Table 2
Characterization of catchment area today and during lake highstands

Surface pattern and parameters				Catchment area characterized by specific vegetation provinces (%)			
α	ε	f	z_0 (cm)	Modern		9-k.y. BP time slice	135-k.y. BP time slice
				Actual coverage	Potential coverage	Reconstructed coverage	
(1) Water surfaces							
0.06	0.99	0.97	0.01	0.05	0.05	0.20 (+287%)	0.15 (+192%)
(2) Savanna grassland							
0.25	0.98	0.05	5.0	0.07	0.14	0.10 (−28%)	0.07 (−50%)
(3) Dry woodlands							
0.20	0.96	0.10	10.0	0.20	0.25	0.09 (−62%)	0.17 (−31%)
(4) Pastures and farming							
0.15	0.95	0.30	20.0	0.44	0	0	0
(5) Sclerophyll forests							
0.12	0.96	0.50	30.0	0.08	0.37	0.20 (−46%)	0.20 (−45%)
(6) Afro-montane forests							
0.09	0.96	0.80	50.0	0.13	0.17	0.34 (+96%)	0.37 (+115%)
(7) Afro-alpine heath, bogs							
0.20	0.97	0.30	10.0	0.02	0.02	0.04 (+75%)	0.04 (+67%)

Means for surface patterns	α	ε	f	z_0 (cm)	C_D	α	ε	f	z_0	C_D
Mean, land surfaces (2–7)	0.16	0.96	0.35	22.5	4.0×10^{-3}	0.14	0.96	0.50	32.0	4.4×10^{-3}
Confidence range	± 0.02	± 0.02	± 0.05	± 5.0	0.2×10^{-3}	± 0.02	± 0.02	± 0.05	± 5.0	0.2×10^{-3}

Surface patterns terminology correspond to the mapping of (1) water-covered areas in the catchment of Lake Naivasha and (2–7) six classes of land-surface areas distinguished by predominant vegetation coverage (cf., Jätzold, 1981). Corresponding environmental parameters were derived from empirical data and tables as outlined in Brutsaert (1982) and Schmugge and André (1991). α reflects the surface albedo, ε the surface emissivity, f the soil moisture availability and z_0 corresponds to the roughness length (according to Schmugge and André, 1991, with $C_D = \kappa^2 \ln(z_r/z_0)^{-2}$, with $\kappa = 0.4$ and $z_r = 1.30 \times 10^4$ cm). The portion of the catchment area characterized by a particular vegetation coverage is calculated from raster-based maps. The actual modern vegetation coverage includes changes by human influence, whereas the potential coverage of present-day is hypothetical as predicted by the altitudinal variation of vegetation (Jätzold, 1981; Maitima, 1991). Paleovegetation was inferred from pollen data (Maitima, 1991; Street-Perrott and Perrott, 1993). The difference between modern and past vegetation is expressed as percentage from the potential modern conditions (in brackets).

tion given in Rodhe and Virji (1976), GDS (1994), ISMCS (1995) and KMD (2000). The values for the short- and longwave cloud coefficients, which symbolize the predominant character of clouds in the catchment, were obtained as described in Bookhagen et al. (2001) (Table 3).

In contrast to the climatological parameters, all environmental parameters depending on surface characteristics, such as emissivity, soil moisture availability, albedo and surface roughness, were compiled for water-covered and land-surface regions separately (Fig. 4). Six classes of different surface patterns were

Table 3
Summary of all input parameters and corresponding modeling results for modern and paleo-Lake Naivasha

Parameter	Units	Modern	9-k.y. BP time slice		135-k.y. BP time slice		Confidence	Ref.
			Without vegetation feedback	With vegetation feedback	Without vegetation feedback	With vegetation feedback		
Catchment area	km^2	3400					± 100	a
Maximum lake level	m a.s.l.	1889	2000 ± 10		1900 ± 10		–	a
Water body	km^3	0.85	59.3		55.4		± 5	a
Lake area	km^2	178.6	684.5		518.5		± 15	a
Portion of basin covered by lake	–	0.052	0.201		0.152		± 0.05	a
Cloudfree shortwave radiation	$W\ m^{-2}$	415					± 3	b
Shortwave cloud parameters	–	0.39, 0.38					–	c
Longwave cloud parameters	–	0.22, 2.0					–	c
Air pressure	Pa	815×10^5					–	d
Cloud coverage	–	0.65	0.65	0.70	0.65	0.70	± 0.05	d
Relative humidity	–	0.65	0.65	0.70	0.65	0.70	± 0.05	d
Windspeed	$m\ s^{-1}$	2.5	2.5	2.8	2.5	2.8	± 0.3	d
Air temperature	°C	13.5	13.5	13.0	13.5	13.0	± 0.5	d
Surface temperature	°C	18.3	18.3	15.7	18.3	15.7	± 0.5	e
Lake-surface water temperature	°C	17.4	17.4	16.1	17.4	16.1	± 0.5	e
Surface drag coefficient	–	4.0×10^{-3}	4.0×10^{-3}	4.4×10^{-3}	4.0×10^{-3}	4.4×10^{-3}	$\pm 0.2 \times 10^{-3}$	f
Surface albedo over water, land	–	0.06, 0.16	0.06, 0.16	0.06, 0.14	0.06, 0.16	0.06, 0.14	± 0.02	f
Surface emissivity over water, land	–	0.99, 0.96	0.99, 0.96	0.99, 0.96	0.99, 0.96	0.99, 0.96	± 0.02	f
Soil moisture over water, land	–	0.97, 0.35	0.97, 0.35	0.97, 0.5	0.97, 0.35	0.97, 0.5	± 0.05	f
Evaporation over water	$mm\ yr^{-1}\ m^{-2}$	1880	1880	1850	1880	1850	± 30	e
Evaporation over land	$mm\ yr^{-1}\ m^{-2}$	915	915	1125	915	1125	± 100	e
Precipitation	$mm\ yr^{-1}\ m^{-2}$	**970**	**1125**	**1280**	**1075**	**1240**	± 100	e
Precipitation including expected basin drainage	$mm\ yr^{-1}\ m^{-2}$	1070	1225	~ 1380	1175	~ 1340	–	g

All input parameters are derived from available climate data sets (see references). Listed values correspond to basin-averaged values, which were obtained by interpolation between weather stations within and in the vicinity of the catchment. Surface-pattern related parameters are derived from vegetation mappings (see text for further explanations). All hydrologic modelings were done in Matlab® using the lake-balance modeling concept published by Blodgett et al. (1997) and Bookhagen et al. (2001). Final modeling results for a steady state of the lake-balance are given in bold letters. Indices reflect: (a) values taken from digital elevation model; (b) Berger and Loutre (1991); (c) Bookhagen et al. (2001); (d) Rodhe and Virji (1976), GDS (1994), ISMCS (1995) and KMD (2000); (e) calculated value for given parameters in the modeling run; (f) surface pattern-related parameters as attributed to vegetation mappings (cf., Table 2); (g) modeled precipitation values including a postulated basin-averaged seepage of $S_{bas} = 100\ mm\ year^{-1}$.

determined, distinguishing between water surfaces, regions covered by afro-alpine heath and bogs, bamboo tree-dominated forests, the sclerophyll forests of *Juniperus* and *Podocarpus*, intensively used areas with pastures and farming, *Acacia*-dominated dry woodland and open savanna land with scattered shrubs and trees (Jätzold, 1981) (Fig. 6). The fraction of the catchment area defined by each surface pattern was calculated from a raster-based mapping of vegetation coverage, where each cell represents an area of 1×1 km. From this mapping, weighting averaged values for albedo, surface roughness, emissivity and soil moisture availability were determined following the principles outlined in Schmugge and André (1991). Basin-averaged albedo $\alpha = 0.16 \pm 0.02$ and surface roughness, reflected by the surface drag coefficient $C_D = 4.0 \pm 0.2 \times 10^{-3}$, represent the predominant savanna-type and deforested environments in the present-day catchment (Jätzold, 1981; Schmugge and André, 1991). Although, nearly 80% of the former sclerophyll forests are cleared for agricultural use, basin-averaged values for emissivity $\varepsilon = 0.96 \pm 0.02$ and soil moisture availability $f = 0.35 \pm 0.05$ are more or less unaffected and reflect prevailing occurrence of water-unsaturated soils (Brutsaert, 1982; Schmugge and André, 1991) (Table 2).

While the majority of all parameters could easily be determined, the amount of subsurface outflow from the lake bottom is a matter of debate. Gaudet and Melack (1981) and Ojiambo-Bwire and Lyons (1996) use such a subsurface outflow as a partial explanation for the low alkalinity of the lake. Assuming, about 36 million m^3 of the direct water loss from Lake Naivasha is contributed to seepage, they also postulate an even higher value for precipitation in the hydrologic budget of the lake. Consequently, the given basin-averaged precipitation varies between 900 and 1100 mm $year^{-1}$ (Griffiths, 1972; Ojany and Ogendo, 1988; Survey of Kenya, 1991; GDS, 1994; ISMCS, 1995; KMD, 2000). In the present-day hydrologic simulation, we used a basin-averaged value of 100 mm $year^{-1}$ reflecting the entire basin seepage, although this value is only attributed to subsurface outflow in the lake area itself.

Applying the input parameters for the present-day conditions (Table 3), the model computes a hypothetical lake precisely at the modern level of Lake Naivasha at 1890 m (Fig. 7). The modeled evaporation rates were 1880 ± 30 mm $year^{-1}$ over open water, but 915 ± 100 mm $year^{-1}$ over land. In order to maintain a stable lake level, the value of precipitation has to reach 970 ± 100 mm $year^{-1}$. This value increases to about 1070 mm $year^{-1}$, as soon as the model allows a significant subsurface outflow as suggested by Ojiambo-Bwire and Lyons (1996).

Intense sensitivity testing of our results was done for the model-input parameters such as solar radiation, temperature, cloud coverage, relative humidity, wind

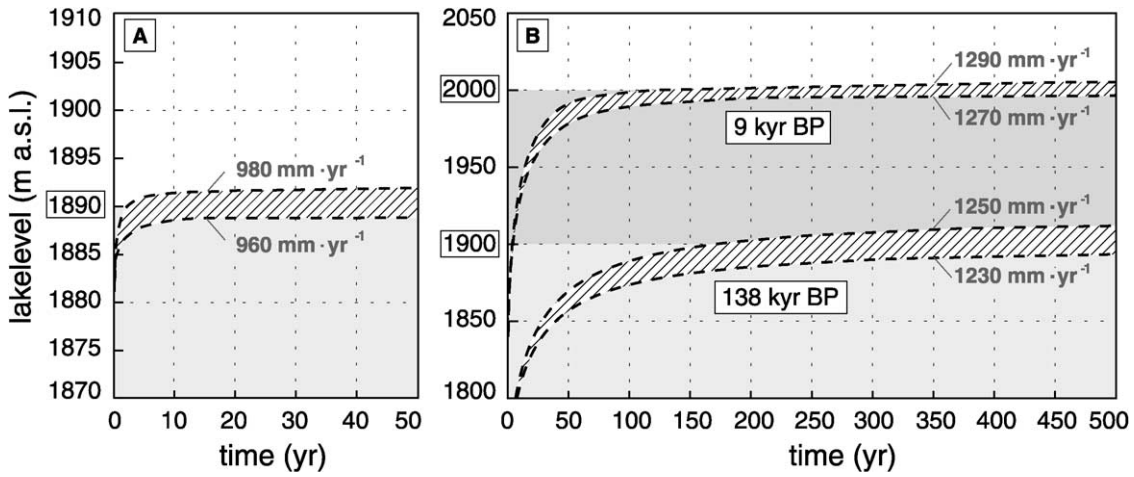

Fig. 7. Modeled lake-fill curves for (A) the modern lake reaching the 1890-m contour and (B) the paleo-lakes at 2000 m (9 k.y. BP) and 1900 m (135 k.y. BP).

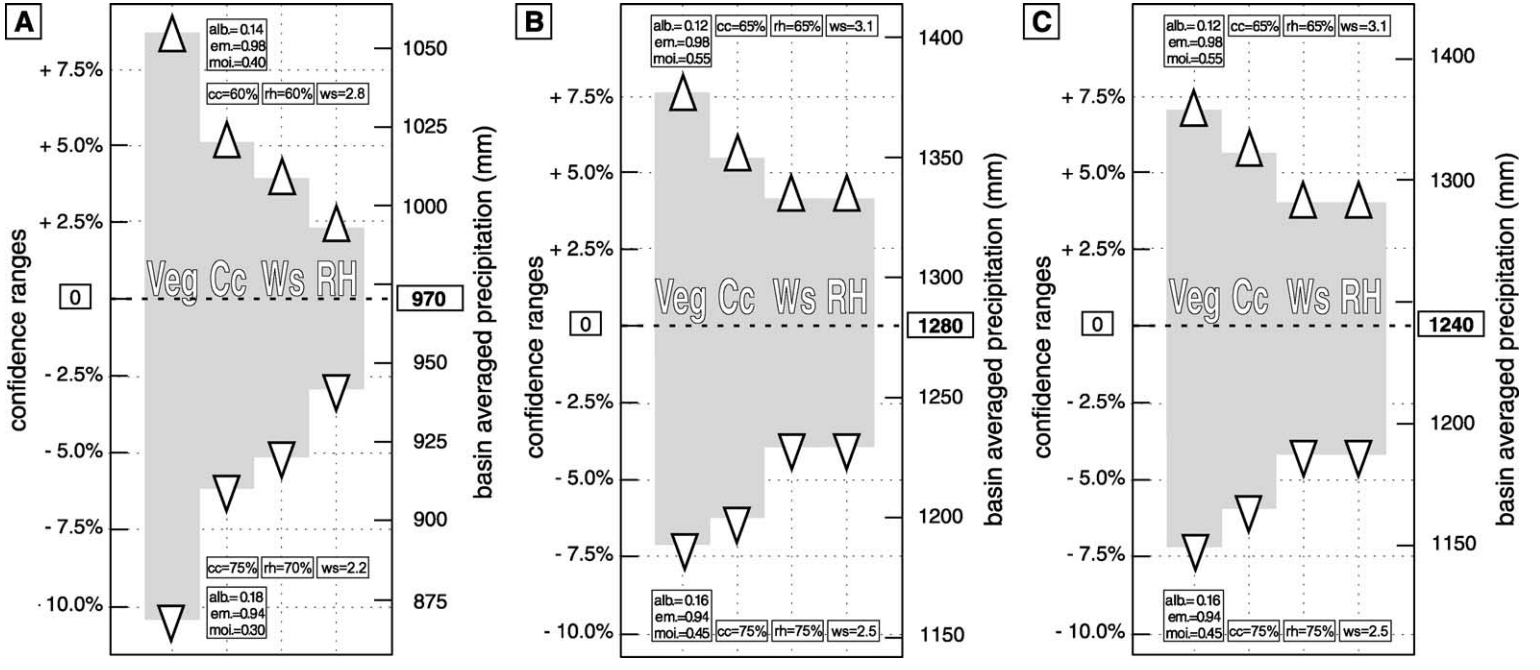

Fig. 8. Results of sensitivity tests for model parameters with important impact on the final result; veg: vegetation coverage, cc: cloud coverage, ws: wind speed, rh: relative humidity. Fluctuations in vegetation coverage introduce larger changes in the modeled precipitation values as compared to all other parameters. In the paleomodeling, the higher portion of water-covered areas reduces the influence of vegetation, whereas all general climatic parameters, i.e., cloud coverage, wind speed and relative humidity, show higher degrees of uncertainty.

speed and the surface-drag coefficient. The influence of each single coefficient was expressed as the deviation of the inferred rainfall value from the modern precipitation estimate. Considering the confidence of the coefficients and their natural variability, the sensitivity tests yield an uncertainty of the modeled precipitation between 2.5% and 10%. Whereas surface roughness is of particular importance, introducing large uncertainties, cloud coverage, wind speed and relative humidity are less important for the final result (Fig. 8). Summing up all uncertainties in definition of the paleoenvironmental parameters and the natural variability of the modern climate indices, the error in the final results most likely is not more than 15%. Thus, a careful adjustment of the model to the paleoconditions starting from the modern values in small steps leads to reasonable results and provides some valuable informations about the dynamics and sensitivity of the lake system.

6. Modeling the paleolake highstands

First, we tried to model the late Pleistocene and early Holocene lakes using the modern values for precipitation and evaporation (Table 3). The resulting hypothetical lakes cover an area similar to the modern lake but the volume of the water bodies are 4.5 and 2.3 km^3, respectively, due to the differences in bathymetry. With the selected input parameters, the late Pleistocene lake does not reach the southern basin boundary and rises only up to the 1760 ± 5-m contour, whereas the early Holocene lake reaches 1855 ± 5 m. The enormous discrepancies between the modeled lakes and the reconstructed geometry of the paleolakes imply significant differences in the hydrologic budget and, hence, the climatic boundary conditions of the catchment area.

The most effective mechanism changing the lake hydrology is either higher lateral moisture transport increasing precipitation or reduced basin-averaged temperatures lowering evaporation. Applying these arguments to the modeling, as a first test all environmental parameters were kept at their modern values assuming that the entire change in the hydrologic budget is attributed to a change in rainfall. The simulation of the 135-k.y. BP highstand suggests an increase of 11% rainfall (1075 mm $year^{-1}$), whereas the 9-k.y. BP paleolake can be simulated using an increase of 16% (1125 mm $year^{-1}$) (Table 3).

Such dramatic changes require the adaptation of many other environmental factors, such as wind speed, cloudiness and higher relative humidity. A realistic scenario for the region of the Naivasha basin is an increase of these parameters by 10% according to similar investigations by Kutzbach et al. (1996). Another consequence of higher moisture levels is a significant change in vegetation of the present-day grassland areas. Climate modeling experiments have shown that vegetation feedbacks can dramatically influence local climatic conditions (e.g., Doherty et al., 2000; Renssen and Lautenschlager, 2000; Carrington et al., 2001). Unfortunately, no Pleistocene vegetation reconstructions are available, but pollen analysis covering the Holocene suggests more extensive woodlands, at least for the more elevated parts of the Lake Naivasha catchment (Maitima, 1991; Street-Perrott and Perrott, 1993). Such vegetation changes would have caused a lower surface albedo, higher soil moisture availability, surface emissivity and surface drag coefficient.

Starting from the grid-based mapping of present-day vegetation coverage, we computed a basin-wide interpolation of paleovegetation using the Holocene pollen records (Maitima, 1991; Street-Perrott and Perrott, 1993). Although, this interpolation can only reflect a very rough estimate of the paleovegetation change, it provides important insights into the potential environmental change due to a more humid climate in the Naivasha basin. Whereas the fraction of the catchment area covered by afro-alpine elements, as well as wet montane forests dramatically increased ($+70\%$ to $+100\%$), areas of dry woodlands and savanna habitats were reduced by -30% to -60% (Table 2; Fig. 6). Following the principles outlined by Schmugge and André (1991), surface roughness of the paleo-Naivasha basin was increased to $C_D = 4.4 \pm 0.2 \times 10^{-3}$, whereas basin-averaged albedo was reduced to $\alpha = 0.14 \pm 0.02$. The basin-averaged emissivity was $\varepsilon = 0.96 \pm 0.02$, whereas soil moisture availability reached $f = 0.5 \pm 0.05$.

The Holocene pollen assemblages also indicate a basin-wide temperature reduction (Street-Perrott and Perrott, 1993) that is most likely attributed to the vegetation change rather than insolation changes (Maitima, 1991; Kutzbach et al., 1996; Renssen and Lau-

tenschlager, 2000). Although, the absolute value of this temperature change is not known, large-scale GCM results imply a reduction on the order of -0.5 to -2 °C (deMenocal and Rind, 1993; Jolly et al., 1998). Since, mean annual insolation does not significantly differ from the present-day value, we used a basin-averaged temperature reduction of -0.5 ± 0.5 °C as a realistic model input for the early Holocene simulation as well as for the late Pleistocene model run. Following the same argument, we applied the paleovegetation reconstruction to both time slices (Table 3).

In consideration of all feedback mechanisms, the time to fill the lake basin after a hypothetical abrupt climate change towards the reconstructed conditions would have been longer by a factor of 10 as compared to the present (Fig. 7). The modeled value for the basin-averaged precipitation is 1240 ± 100 mm year^{-1} (+28%) for the 135-k.y. BP lake level, and 1280 ± 100 mm year^{-1} (+32%) for the 9-k.y. BP highstand, respectively. Variations of the input parameters within the defined confidence ranges indicate that changes in the vegetation-controlled parameters introduce a lower degree of uncertainty into the modeling results than during the modern run (Fig. 8). The higher portion of water-covered areas during the paleohighstands reduces the hydrologic influence of vegetation. In contrast, general climatic parameters, i.e., cloud coverage, wind speed and relative humidity, show a higher degree of uncertainty for the paleomodeling results ($\pm 4\%$ to $\pm 6\%$).

Our model runs do not consider changes in the subsurface outflow. However, during the 9-k.y. BP highstand, the lake had at least a temporary overflow through the Ol Njorowa Gorge (Washbourn-Kamau, 1977). As there are good arguments for a subsurface outflow under the present lake, a potential change in the amount of groundwater infiltration was discussed (Gaudet and Melack, 1981; Ojiambo-Bwire and Lyons, 1996; R. Becht, personal communication, 2000). It is assumed that infiltration should have been comparable to its present-day value during the paleolake highstands, or even less due to more water-saturated grounds, higher water tables and lower groundwater gradients. Although, exact values of the overflow and subsurface outflow are unknown, the modeled values for paleoprecipitation for both highstands are believed to be minimum estimates.

7. Paleoclimate implications

The dimension of Lake Naivasha during the two highstands at 135 and 9 k.y. BP compared to present illustrates the extreme variability of climate and hydrology in the Central Kenya Rift. Since the Naivasha basin was not affected by important tectonic movements or volcanic activity during the last 175 k.y., the observed lake-level fluctuations document long-term changes in the precipitation/evaporation balance. Our modeling results suggest that precipitation was increased by 11–16% compared to the present-day value. Starting from the modern climate conditions, such an increase in humidity would result in a stable lake at the reconstructed level after a minimum time of 200 years. This change toward more humid conditions, however, would also cause changes in vegetation in the catchment. If the adaptation and migration of vegetation and subsequent higher transpiration are introduced into the model, the hydroclimatic conditions in the catchment would be characterized by a 28–32% increase in mean annual precipitation. A change in the amount of subsurface outflow from the lake would lead to further changes in the paleohydrologic budget; but since no strong arguments support such changes, our modeling results reflect minimum, but realistic estimates of the precipitation/evaporation change.

For the early Holocene climate optimum, our modeling results are in the same order of magnitude as climate parameters modeled by Hastenrath and Kutzbach (1983) for this region. The authors use a more generalized energy budget method and found a minimum precipitation change of 10% in the catchment. Vegetation changes in the cause of such a more humid climate would increase this value to 17% (Hastenrath and Kutzbach, 1983). In contrast, Vincent et al. (1989) found a 350-mm year^{-1} (+55%) increase in rainfall, similar to the results from GCM experiments (deMenocal and Rind, 1993) and run-off calculations by Butzer et al. (1972). However, these results seem to overestimate the regional precipitation changes because they do not take into account the large spatial heterogenities in rainfall in the Central Kenya Rift. Our grid-based lake-balance model allows a precise assessment of local rainfall anomalies and large gradients in the environmental parameters. The modeled precipitation changes of 16–32%

are, therefore, believed to be a better estimate for the true paleoclimatic conditions in the Central Kenya Rift.

In contrast to the detailed paleoclimatic information for the Early Holocene, climate records for the late Pleistocene are scarce (Richardson and Richardson, 1972; Trauth et al., 2001). The history of Lake Naivasha suggests that although the causes for the highstands at 135 and 9 k.y. BP were different (Richardson and Dussinger, 1986; Trauth et al., 2001), the hydroclimatic conditions in the Naivasha basin during these highstands show significant similarities. Whereas the 135-k.y. BP highstand seems to be the result of maximum March insolation on the equator resulting in a strong intertropical convergence and high precipitation during the April/May rains (Trauth et al., 2001), the 9-k.y. BP highstand correlates with maximum Northern Hemisphere insolation and a strong summer monsoonal circulation (Richardson and Dussinger, 1986; Gasse, 2000). Herein, a stronger influence of westerly flows may be speculated. However, an important factor for both highstands seems to be higher intraannual fluctuations in air temperature. More precipitation during the rainy seasons and decreased evaporation during the dry season would result in a more positive net moisture budget in the course of a year.

The magnitude of the hydrologic changes in the Naivasha basin provides valuable insights into the sensitivity of this natural system. Obviously, the present-day character of the modern lake only represents a snapshot of its natural variability and the climate system. As demonstrated by our modeling, a relatively small change in humidity can rise the lake level from less than 10 to more than 100 m, an area three times larger would be flooded by water. Paleoclimatic reconstructions from other basins suggest, that high and large lakes are a common feature in East Africa at least during the Early Holocene (Street-Perrott and Perrott, 1993; Jolly et al., 1998; Gasse, 2000). During this time, open water surfaces or papyrus swamps covered most of the inner graben region. These dramatic environmental changes certainly had important consequences and feedbacks on regional, but maybe also for global climates. Such relationships between East African climate and the global implications should be the subject for future large-scale GCM experiments.

Acknowledgements

This project was funded by two grants to M. Trauth and M. Strecker by the German Research Foundation (DFG). We thank the government of Kenya and the Kenya Wildlife Service for research permits and support. We also thank R. Becht, P. Blisniuk, F. Chalié, M. Dühnforth, M. Edwards, A. Friedrich, S. Gaciri, F. Gasse, K. Haselton, R. Hennemann, G. Muchemi, M. Strecker, C. Vallet-Coulomb, D. Verschuren and Z. Liu for discussions. We also thank S. and M. Higgins for providing core log data and their support during fieldwork in the Naivasha basin. T. Schlüter and M. Ibs-von Seht are acknowledged for their logistical support.

References

Åse, L.-E., 1987. A note on the water budget of Lake Naivasha. Geographiska Annaler 69A, 415–429.

Baker, B.H., Wohlenberg, J., 1971. Structure and evolution of the Kenya Rift Valley. Nature 229, 538–542.

Barker, P.A., Street-Perrott, F.A., Leng, M.J., Greenwood, P.B., Swain, D.L., Perrott, R.A., Telford, R.J., Ficken, K.J., 2001. A 14,000-year oxygen isotope record from diatom silica in two alpine lakes on Mt. Kenya. Science 292, 2307–2310.

Barron, E.J., Moore, G.T., 1994. Climate Model Applications in Paleoenvironmental Analysis Society for Sedimentary Geology, Tulsa, USA.

Berger, A., Loutre, M.F., 1991. Insolation values for the climate of the last 10 million years. Quaternary Science Reviews 10 (4), 297–317.

Blodgett, T.A., Lenters, J.D., Isacks, B.L., 1997. Constraints on the origin of paleolake expansions in the central Andes available online at (http://www.earthinteractions.org).

Bone, B.D., 1985. The geological evolution of the S.W. Naivasha volcanic complex, Kenya. PhD thesis, University of Lancaster, UK.

Bookhagen, B., Haselton, K., Trauth, M.H., 2001. Hydrological modeling of a landslide-dammed lake in the Santa Maria basin, NW Argentina. Palaeogeography, Palaeoclimatology, Palaeoecology 169 (1–2), 113–127.

Bosworth, W., Strecker, M., 1997. Stress field changes in the Afro-Arabian rift system during the Miocene to recent period. Tectonophysics 278, 47–62.

Brutsaert, W., 1982. Evaporation into the Atmosphere. D. Reidel Publishing, Dortrecht.

Butzer, K.W., Isaac, G.L., Richardson, J.L., Washbourn-Kamau, C., 1972. Radiocarbon dating of East African lake levels. Science 175, 1069–1076.

Carrington, D.P., Gallimore, R.G., Kutzbach, J.E., 2001. Climate sensitivity to wetlands and wetland vegetation in mid-Holocene North Africa. Climate Dynamics 17, 151–157.

Clarke, M.C.G., Woodhall, D.G., Allen, D., Darling, G., 1990. Geological, volcanological and hydrogeological controls on the occurrence of geothermal activity in the area surrounding Lake Naivasha, Kenya. British Geological Survey Report and Government of Kenya—Ministry of Energy, Nairobi, Kenya.

deMenocal, P.B., Rind, D., 1993. Sensitivity of Asian and African climate to variations in seasonal insolation, glacial ice cover, sea surface temperature and Asian orography. Journal of Geophysical Research 98, 7265–7287.

deNoblet, N., Braconnot, P., Joussaume, S., Masson, V., 1996. Sensitivity of simulated Asian and African monsoons to induced variations in insolation 126, 115 and 6 kBP. Climate Dynamics 12, 589–603.

Doherty, R., Kutzbach, J., Foley, J., Pollard, D., 2000. Fully coupled climate/dynamical vegetation model simulations over Northern Africa during the mid-Holocene. Climate Dynamics 16 (8), 561–573.

Dong, B., Valdes, P.J., Hall, N.M.J., 1996. The changes of monsoonal climates due to earth's orbital perturbations and ice age boundary conditions. Paleoclimates 1, 203–240.

Gasse, F., 2000. Hydrological changes in the African tropics since the Last Glacial Maximum. Quaternary Science Reviews 19, 189–211.

Gasse, F., Lédée, V., Massault, M., Fontes, J.C., 1989. Water-level fluctuations of Lake Tanganyika in phase with oceanic changes during the last glaciation and deglaciation. Nature 342, 57–59.

Gaudet, J.J., Melack, J.M., 1981. Major ion chemistry in a tropical lake basin. Freshwater Biology 11, 309–333.

Global Daily Summary (GDS)—Temperature and Precipitation, CD-Rom Vers. 1.0, 1994. Federal Climate Complex Asheville, National Oceanic and Atmospheric Administration, Department of Commerce, Washington, USA.

Griffiths, J.F., 1972. Climates of Africa. World Survey of Climatology, vol. 10. Elsevier, Amsterdam.

Hastenrath, S., Kutzbach, J.E., 1983. Paleoclimatic estimates from water and energy budgets of East African Lakes. Quaternary Research 19, 141–153.

International Station Meteorological Climate Summary (ISMCS), CD-Rom Vers. 3.0, 1995. Federal Climate Complex Asheville, National Oceanic and Atmospheric Administration, Department of Commerce, Washington, USA.

Jätzold, R., 1981. Klimageographie—Ostafrika, Kenya, Uganda, Tanzania 2°N–2°S, 32–38°E. In: Freitag, U. (Ed.), Afrika-Kartenwerk, Serie E. Beiheft zu Blatt, vol. 5. Bornträger, Berlin, pp. 1–129.

Johnson, T.C., Kelts, K., Odada, E., 2000. The Holocene history of Lake Victoria. Ambio 29 (1), 2–11.

Jolly, D., Harrison, S.P., Damnati, B., Bonnefille, R., 1998. Simulated climate and biomes of Africa during the Late Quaternary: comparison with pollen and lake status data. Quaternary Science Reviews 17, 629–657.

Kenya Meteorological Department, 2000. Unpublished synoptic and rain station data. Ministry of Information, Transport and Communications, Nairobi, Kenya.

Kutzbach, J.E., Webb III, T., 1993. Conceptual basis for understanding Late-Quaternary climates. In: Wright Jr., H.E. (Ed.), Global Climates Since the Last Glacial Maximum. University of Minnesota Press, Minnesota, pp. 5–11.

Kutzbach, J., Bonan, G., Foley, J., Harrison, S.P., 1996. Vegetation and soil feedbacks on the response of the African monsoon to orbital forcing in the early to middle Holocene. Nature 384, 623–626.

Maitima, J.M., 1991. Vegetation response to climatic change in Central Rift Valley, Kenya. Quaternary Research 35, 234–245.

Nicholson, S.E., 1996. A review of climate dynamics and climate variability in Eastern Africa. In: Johnson, T.C., Odada, E. (Eds.), The Limnology, Climatology and Paleoclimatology of the Eastern African Lakes. Gordon & Breach Publishers, Amsterdam, pp. 549–557.

Nicholson, S.E., Yin, X., 2001. Rainfall conditions in equatorial East Africa during the Nineteenth century as inferred from the record of Lake Victoria. Climatic Change 48, 387–398.

Ojany, F.F., Ogendo, R.B., 1988. A Study in Physical and Human Geography Longman, Nairobi, Kenya.

Ojiambo-Bwire, S., Lyons, W.B., 1996. Residence of major ions in Lake Naivasha and their relationship to lake hydrology. In: Johnson, T.C., Odada, E. (Eds.), The Limnology, Climatology and Paleoclimatology of the Eastern African Lakes. Gordon & Breach Publishers, Amsterdam, pp. 267–278.

Onacha, S.A., 2000. Use of electrical resistivity methods to evaluate the hydrogeology of the Lake Naivasha Basin. In: Ogola, J.S., Behr, H.-J. (Eds.), Saline–Alkaline Lakes in Eastern and Southern Africa, Workshop Proceedings, University of Nairobi, Nairobi, pp. 60–71.

Prell, W.L., Kutzbach, J.E., 1987. Monsoon variability over the past 150,000 years. Journal for Geophysical Research 92 (D7), 8411–8425.

Renssen, H., Lautenschlager, M., 2000. The effect of vegetation in a climate model simulation on the Younger Dryas. Global and Planetary Change 26, 423–443.

Richardson, J.L., Dussinger, R.A., 1986. Paleolimnology of mid-elevation lakes in the Kenya Rift Valley. Hydrobiologia 143, 167–174.

Richardson, J.L., Richardson, A.E., 1972. History of an African Rift Lake and its climate implications. Ecological Monographs 42, 499–534.

Rodhe, H., Virji, H., 1976. Trends and periodicities in East African rainfall data. Monthly Weather Review 104, 307–315.

Sandwell, D.T., 1987. Biharmonic spline interpolation of Geos-3 and Seasat altimeter data. Geophysical Research Letters 14 (2), 139–142.

Schmugge, T.J., Andre, J.C. (Eds.), 1991. Land Surface Evaporation—Measurement and Parameterisation. Springer, New York, 424 pp.

Shuttleworth, W.J., 1988. Parameterization schemes of land-surface processes for mesoscale atmospheric models. In: Schmugge, T.J., André, J.C. (Eds.), Land Surface Evaporation—Measurement and Parameterisation. Springer, New York, pp. 55–92.

Strecker, M., Blisniuk, P., Eisbacher, G., 1990. Rotation of extension direction in the central Kenya Rift. Geology 18, 299–302.

Street-Perrott, F.A., Perrott, R.A., 1993. Holocene vegetation, lake

levels and climate of Africa. In: Wright Jr., H.E., Kutzbach, J.E., Webb III, T., Ruddimann, W.F., Street-Perrott, F.A., Bartlein, P.J. (Eds.), Global Climates since the Last Glacial Maximum. University of Minnesota Press, Mineapolis, pp. 318–356.

Survey of Kenya, 1991. National Atlas of Kenya, 4th ed. Kenya Government, Nairobi, Kenya.

Talbot, M.R., Lærdal, T., 2000. The Late Pleistocene-Holocene palaeolimnology of Lake Victoria, East Africa, based upon elemental and isotopic analyses of sedimentary organic matter. Journal of Paleolimnology 23, 141–164.

Thompson, A.D., Dodson, R., 1963. Geology of the Naivasha Area. Geological Survey of Kenya Report 55, Nairobi, Kenya.

Trauth, M.H., Strecker, M.R., 1996. Late Pleistocene lake level fluctuations in the Naivasha basin, Kenya. In: Johnson, T.C., Odada, E. (Eds.), The Limnology, Climatology and Paleoclimatology of the Eastern African Lakes. Gordon & Breach Publishers, Amsterdam, pp. 549–557.

Trauth, M.H., Deino, A., Strecker, M.R., 2001. Response of the East African climate to orbital forcing during the last interglacial (130–117 ka) and the early last glacial (117–60 ka). Geology 29, 499–502.

Verschuren, D., Laird, K.R., Cumming, B.F., 2000. Rainfall and drought in equatorial Africa during the past 1100 years. Nature 403, 410–413.

Vincent, C.E., Davies, T.D., Beresford, A.K.C., 1979. Recent changes in the level of Lake Naivasha, Kenya, as an indicator of equatorial westerlies over East Africa. Climatic Change 2, 175–189.

Vincent, C.E., Davies, T.D., Primblecombe, P., Beresford, A.K.C., 1989. Lake levels and glaciers: indicators of the changing rainfall in the mountains of East Africa. In: Mahaney, W.C. (Ed.), Quaternary and Environmental Research on East African Mountains. York University, North York, Canada, pp. 199–216.

Washbourn-Kamau, C.K., 1975. Late Quaternary shorelines of Lake Naivasha, Kenya. Azania X, 77–92.

Washbourn-Kamau, C.K., 1977. The Ol Njorowa Gorge, Lake Naivasha basin, Kenya. In: Greer, D.C. (Ed.), Desertic Terminal Lakes. Utah Water Research Laboratory, Utah State University, Logan, pp. 297–307.

Wessel, P., Bercovici, D., 1998. Interpolation with splines in tension: a Green's function approach. Mathematical Geology 30 (1), 77–93.